Planetary and Space Science xxx (2017) 1–9

Contents lists available at ScienceDirect

Planetary and Space Science

journal homepage: www.elsevier.com/locate/pss

Impact cratering on porous targets in the strength regime

Akiko M. Nakamura

Graduate School of Science, Kobe University, 1-1 Rokkodai-cho, Nada-ku, Kobe 657-8501, Japan

ARTICLE INFO

Keywords:
Crater
Dust
Impact experiment
Porosity
Small body

ABSTRACT

Cratering on small bodies is crucial for the collision cascade and also contributes to the ejection of dust particles into interplanetary space. A crater cavity forms against the mechanical strength of the surface, gravitational acceleration, or both. The formation of moderately sized craters that are sufficiently larger than the thickness of the regolith on small bodies, in which mechanical strength plays the dominant role rather than gravitational acceleration, is in the strength regime. The formation of microcraters on blocks on the surface is also within the strength regime. On the other hand, the formation of a crater of a size comparable to the thickness of the regolith is affected by both gravitational acceleration and cohesion between regolith particles.

In this short review, we compile data from the literature pertaining to impact cratering experiments on porous targets, and summarize the ratio of spall diameter to pit diameter, the depth, diameter, and volume of the crater cavity, and the ratio of depth to diameter. Among targets with various porosities studied in the laboratory to date, based on conventional scaling laws (Holsapple and Schmidt, *J. Geophys. Res.,* 87, 1849–1870, 1982) the cratering efficiency obtained for porous sedimentary rocks (Suzuki et al., *J. Geophys. Res.* 117, E08012, 2012) is intermediate. A comparison with microcraters formed on a glass target with impact velocities up to 14 km s^{-1} indicates a different dependence of cratering efficiency and depth-to-diameter ratio on impact velocity.

1. Introduction

Mass ejection by cratering has been found to be crucial in collision cascades which are one of the most important processes in the main asteroid belt, the Edgeworth-Kuiper Belt, debris disks, and planet formation (Kobayashi and Tanaka, 2010). Cratering on small bodies contributes to the ejection of dust particles into interplanetary space (Yamamoto and Mukai, 1998; Tomeoka et al., 2003). During high-velocity impact on the surface of a planetary body, a crater cavity is excavated against the mechanical strength of the surface, the gravitational acceleration, or both (Holsapple, 1993). When the surface has a porous structure, cavity formation also proceeds by compaction of that structure (Housen and Holsapple, 2003). In other words, the response of a planetary surface to impact depends on its physical properties, such as mechanical strength, porosity, and internal structure (Nakamura et al., 2009), and on its gravitational acceleration.

The size of a relatively large crater is limited mainly by gravitational acceleration, rather than by mechanical strength. This situation is called the gravity regime. Even when a small crater is created, if the mechanical strength is negligible, such as when a millimeter-size projectile impacts a sand target in the laboratory, the size of the crater cavity is dependent mainly on gravitational acceleration. On the other hand, when the effect of gravity is negligible compared with the mechanical strength, the impact process and its consequences, such as the dimensions and shape of the cavity, are in the strength regime and depend on the material strength, porosity, and structural characteristics such as the density structure or spatial inhomogeneity. In the laboratory, the speed of cratering ejecta has been shown to be related to the mechanical strength of the surface, i.e., the stronger the target, the higher the ejecta speed (Housen, 1992; Michikami et al., 2007; Housen and Holsapple, 2011). Cratering efficiency is affected by the size ratio between the projectile and the target grain when the projectile size is so small that the disruption of the single target grain by the projectile is not negligible (Guettler et al., 2012).

The appearance of craters on small bodies differs markedly among different types of bodies. Large craters, with diameters comparable to the diameter of the asteroid, coexist on the asteroid 253 Mathilde (Veverka et al., 1999). The reason why such large craters can coexist, and why the body was not disrupted or dispersed, is probably that the porosity effectively attenuated the shock pressure via compaction (Housen et al., 1999; Housen and Holsapple, 2003). Ejecta blocks of tens of meters to ~100 m in size have been found in the vicinity of craters on Martian moons (Lee et al., 1986) and asteroid 243 Ida (Lee et al., 1996), and are even widespread over the surface of asteroid 433 Eros (Thomas et al.,

E-mail address: amnakamu@kobe-u.ac.jp.

http://dx.doi.org/10.1016/j.pss.2017.09.001
Received 31 January 2017; Received in revised form 26 August 2017; Accepted 7 September 2017
Available online xxxx
0032-0633/

2001). However, no ejecta blocks have been identified on Mathilde (Veverka et al., 1999), this is attributed to the high porosity of the body (Housen and Holsapple, 2012). Ejecta blocks that are meters to tens of meters in size are more prominent on the rubble-pile asteroid 25143 Itokawa (Michikami et al., 2008), where typical bowl-shaped craters have not been identified but very shallow circular depressions have been observed (Hirata et al., 2009).

As shown in Section 2, craters that are tens to hundreds of meters in size on a ~1-km diameter body such as asteroid 162173 Ryugu, the mission target of Hayabusa2, can be affected markedly by the mechanical strength, porosity, and structure of the surface. Microcraters on blocks and even on the regolith particles on the surface of small bodies also form in the strength regime. Most small solar system bodies are porous, which means, that the bulk density of the bodies is smaller than those of the component materials of the bodies such as chondrites (Consolmagno et al., 2008). The *S*-type asteroid Itokawa has been shown to be a rubble-pile, i.e., a re-accumulated body, and has a macroporosity of 40% according to the results from Hayabusa (Fujiwara et al., 2006). The *C*-type asteroid Mathilde has also been explored by the space mission NEAR Shoemaker. The bulk density of this body, 1300 kg m^{-3}, shows that its macroporosity is about 50% (Veverka et al., 1999). Moreover, chondrites are also porous, i.e., ordinary chondrites have a porosity of several to tens of percent and carbonaceous chondrites are more porous (Consolmagno et al., 2008).

Here we review laboratory high-velocity impact experiments performed to study the dimensions and shapes of craters on brittle targets, especially on porous targets. In Section 2, the size of craters expected to be produced in the strength regime is roughly defined. In Section 3, laboratory experiments on the dimensions and shapes of craters on brittle targets, with a focus on porous targets, are summarized. Recent laboratory experiments have been conducted using millimeter-to centimeter-size projectiles, resulting in craters ranging in diameter from centimeters to tens of centimeters. However, microcraters have been found on lunar samples, as well as on samples returned from asteroid Itokawa (Nakamura et al., 2012; Matsumoto et al., 2016; Harries et al., 2016); therefore, craters with diameters smaller than 1 mm are also of interest. Hence, we also refer to the results of previous laboratory impact experiments investigating microcraters and make a comparison between microcraters and centimeter-scale craters formed in the laboratory.

2. Size of craters on small bodies in the strength-dominated regime

The gravity-strength transition diameter of the crater regime can be estimated roughly by balancing the mechanical strength of the surface Y and the lithostatic pressure, ρgl, where ρ, g, and l are the density of the surface, the gravitational acceleration, and the representative scale in terms of crater dimensions, respectively. If we take the crater diameter as the representative scale, the transition diameter D_{tr} satisfies the relationship

$$Y = k_1 \rho g D_{tr}, \tag{1}$$

where k_1 is a factor. Substituting $g = G\rho \frac{4\pi}{3} R$, where R is the radius of a spherical body, yields

$$Y = k_1 \rho \left(G\rho \frac{4\pi}{3} R \right) D_{tr}. \tag{2}$$

Accordingly, the relationship of the transition diameter versus the radius of the body is given as

$$D_{tr} = \frac{3Y}{4k_1 \pi G \rho^2 R}. \tag{3}$$

Note that a thorough analysis of the cratering process based on a point source assumption shows that the transition between strength and gravity regimes depends on the impact velocity and occurs at $Y \approx \rho g a$, where a is the impactor radius (Holsapple, 1993) and derives a functional form for the transition involving impact velocity (e.g., Housen and Holsapple, 2011).

Fig. 1 shows the crater diameter of the gravity-strength transition according to Eq. (3). For example, craters smaller than ~18 km in diameter on an 18-km-diameter body having a mechanical strength of 0.1 MPa and density of 1500 kg m^{-3} can form in the strength regime, if k_1 is unity or less. However, the surface of a body is generally covered by regolith. For example, the thicknesses of the regolith on Eros and Phobos have been estimated to be tens of meters (Thomas et al., 2001) and 5–100 m (Basilevsky et al., 2014), respectively. Given that the nominal depth-to-diameter ratio of a bowl-shaped crater is 0.2 (Pike, 1974), craters with diameter D in the following range can be considered to have formed in the strength regime.

$$5h \ll D < D_{tr}, \tag{4}$$

where h is the thickness of regolith layer.

Regolith particles are produced by impact (Housen and Wilkening, 1982) and by thermal fatigue (Delbo et al., 2014). Here, we consider only production by impact. To obtain a first-order estimate of regolith thickness, we assume that impact cratering occurs on a consolidated surface and fragments the surface materials, and that a portion of the disaggregated materials re-accumulates and becomes distributed uniformly over the entire surface of the spherical body. The size distribution of the ejecta particles and the erosion of pre-existing regolith materials by impact are not taken into consideration. Then the average regolith thickness $h(D)$ owing to a crater of diameter D is given by

$$h(D) = \frac{M(D)}{4\pi R^2 \rho_{regolith}}, \tag{5}$$

where $M(D)$ is the mass of re-accumulated ejecta and $\rho_{regolith}$ is the bulk density of the regolith layer. The bulk density of the regolith layer is

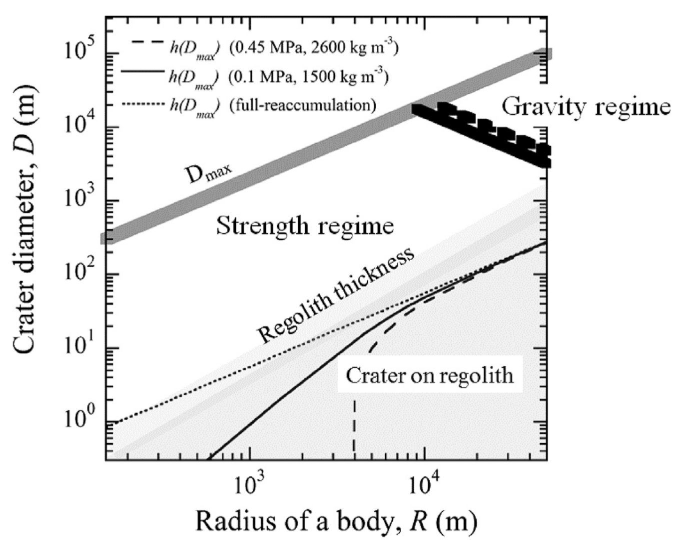

Fig. 1. Diameter range of craters in the strength regime which is restricted below the gravity-strength transition indicated by the thick solid line (Y = 0.1 MPa, ρ = 1500 kg m^{-3}, k_3 = 1 in Eq. (3)) and the thick dashed line (Y = 0.45 MPa, ρ = 2600 kg m^{-3}, k_3 = 1 in Eq. (3)) and the maximum crater diameter, D_{max}, and above the thickness of regolith. The thin solid line and thin dashed line indicate the average regolith thickness owing to the largest crater for a material of Y = 0.1 MPa, ρ = 1500 kg m^{-3}, and the empirical function of escape fraction of ejecta presented in Michikami et al. (2008) and for the one of Y = 0.45 MPa, ρ = 2600 kg m^{-3}, and Eq. (10) with the parameter set of weak cemented basalt, C_s = 0.122 and β_s = 1.38, respectively, although the value of C_s was derived based on an advanced ejecta model (Housen and Holsapple, 2011) and not on a simple power-law assumed here. The thin dotted line shows the upper limit derived by assuming complete re-accumulation of the ejecta.